Combination of quercetin and hyperoside inhibits prostate cancer cell growth and metastasis via regulation of microRNA-21

FENG-QIANG YANG*, MIN LIU*, WEI LI, JIAN-PING CHE, GUANG-CHUN WANG and JUN-HUA ZHENG

Department of Urology, Shanghai Tenth People's Hospital, Tongji University, Shanghai 200072, P.R. China

Received January 30, 2014; Accepted October 1, 2014

DOI: 10.3892/mmr.2014.2813

Abstract. Previous studies have reported that hyperoside and quercetin in combination (QH; 1:1) inhibited the growth of human leukemia cells. The aim of the present study was to investigate the anti-cancer effect of QH on prostate cancer cells. The results demonstrated that QH decreased the production of reactive oxygen species (ROS) and increased antioxidant capacity in PC3 cells at various concentrations (2.5-60 μg/ml) with peak inhibition and augmentation changes of 3.22- and 3.00-fold, respectively. Following treatment with QH for 48 and 72 h, the IC_{50}-values on PC3 cells were 19.7 and 12.4 μg/ml, respectively. Western blot analysis revealed that QH induced apoptosis in human prostate cancer cells via activation of caspase-3 and cleavage of poly(adenosine diphosphate ribose) polymerase. In addition, QH significantly inhibited the invasion and migration of PC3 cells as well as reduced the expression of numerous prostate tumor-associated microRNAs (miRs), including miR-21, compared to that of untreated human prostate cancer cells. QH was also found to enhance the expression of tumor suppressor programmed cell death protein 4, which was negatively regulated by miR-21. Furthermore, induced overexpression of miR-21 using pre-miR-21 oligonucleotides attenuated the beneficial effect of QH on prostate cancer cells. In conclusion, the results of the present study indicated that QH exerted an anti-cancer effect on human prostate cancer cells, the mechanism of which proceeded, at least in part, via the inhibition of the miR-21 signaling pathway.

Introduction

Prostate cancer, as the second most prevalent cause of cancer-associated mortality in males in the USA, accounts for ~30% of malignant tumors in males, affecting one in six and causing mortality in 1 in 35 males (1). Prostate cancer, if diagnosed in the early stages of the disease, may be successfully treated using surgical resection and radiation therapy; however, the majority of patients are diagnosed with locally advanced or metastatic prostate cancer, which requires hormone ablation therapy (2). Following initiation of hormone ablation therapy, ~80-90% of patients develop metastatic castration-resistant prostate cancer (CRPC) within 12-33 months (3). CRPC is currently treated using chemotherapeutic drugs; however, these drugs are unspecific and have numerous adverse effects (4). Therefore, novel therapeutic strategies as well as prophylactic measures are required.

A diet rich in fruits and vegetables has been reported to have protective effects against chronic degenerative diseases, including numerous types of cancer and cardiovascular diseases; the mechanisms underlying these beneficial effects were attributed to plant-derived compounds, such as polyphenols (5). Quercetin is a dietary flavonoid found in tea, onions, grapes, wines and apples, and the anti-cancer activities of this compound have been previously explored in breast and colon cancer cells (6,7). Tang *et al* (8) reported that quercetin and epigallocathechin gallate synergistically inhibited invasion, migration and epithelial mesenchymal transition in prostate cancer stem cells; another study demonstrated that quercetin and sulforaphane synergistically inhibited self-renewal in pancreatic cancer stem cells (9). Hyperoside (quercetin-3-O-galactoside) is a flavonoid compound, which is primarily extracted from *Hypericum perforatum* L (10). Hyperoside was reported to exhibit anti-cancer effects via inhibition of cell proliferation, induction of apoptosis, decreased angiogenesis and induction of cell cycle arrest in numerous cancer cell lines (11). Another previous study demonstrated that the combination of hyperoside and quercetin exhibited synergistic inhibitory effects on the growth of human leukemia cells (12). In a study using mouse skin tumors, a combination of hyperoside and tea polyphenols also demonstrated synergistic anti-cancer effects (13).

Micro (mi)RNAs are small non-coding single-stranded RNAs composed of 22 nucleotides, which regulate coding RNAs at the post-transcriptional level. A single miRNA controls hundreds of target messenger (m)RNAs and miRNAs are therefore powerful transcription factors which may regulate whole cell proteomes (14). miRNAs have become the focus of an increasing number of studies due to the reported roles of

Correspondence to: Professor Jun-Hua Zheng, Department of Urology, Shanghai Tenth People's Hospital, Tongji University, 301 Yanchang Mid-Road, Yangpu, Shanghai, 200072, P.R. China
E-mail: kidneyliu@163.com

*Contributed equally

Key words: quercetin, hyperoside, prostate cancer, microRNA-21

miRNAs in influencing cancer biology, including proliferation, apoptosis and invasive capacity. miR-21 was reported to regulate the growth of breast cancer MCF7 cells *in vitro* and in xenograft mouse models *in vivo* (15). Subsequent studies demonstrated that miR-21 regulated breast cancer metastasis via the downregulation of tumor suppressor genes, including maspin and programmed cell death protein 4 (PDCD4) (16). In addition, miR-21 was reported to regulate glioblastoma intravasation and metastasis through the targeted downregulation of PDCD4 (17). Therefore, the aim of the present study was to evaluate the combined treatment of prostate carcinoma cells with hyperoside and quercetin in order to investigate its effect on PDCD4 expression and the potential involvement of miR-21 in the downregulation of PDCD4 transcription factors.

Materials and methods

Botanical extract. Polyphenols were extracted from a standardized hyperoside and quercetin dihydrate supplement (ratio, 1:1) in capsule form, which was obtained from Jiangsu Suzhong Pharmaceutical Group Co., Ltd (Jiangsu, China). Polyphenols were extracted using 50 mg/ml methanol (Sigma-Aldrich, St. Louis, MO, USA), followed by centrifugation at room temperature for 10 min at 1,100 x g in order to remove inactive and insoluble components. Methanol was evaporated in a rotavapor (BÜCHI Labortechnik AG, Flawil, Switzerland) at 40˚C. Residual moisture was evaporated using a speedvac concentrator (Thermo Scientific, Waltham, MA, USA) at 43˚C. The final mixture of hyperoside and quercetin in combination (QH) was stored at -80˚C and dissolved in dimethyl sulfoxide (Sigma-Aldrich) prior to use.

High-performance liquid chromatography photo-diode array (HPLC-PDA) analysis. The polyphenolic mixture was analyzed and quantified by retention time and PDA spectra using HPLC-PDA. Chromatographic separation was performed in an Alliance 2695 Seperations Module (Waters Corp., Milford, MA, USA) using a Discovery® C18 column (Supelco; 250x4.6 mm, 5 μm; Sigma-Aldrich) at room temperature. The chromatographic conditions used were as follows: Mobile phase A, water/acetic acid (Sigma-Aldrich) 98:2; mobile phase B, acetonitrile/water/acetic acid 68:30:2. A gradient program with a flow rate of 1 ml/min was used as follows: 0 min, 100% A; 20 min, 60% A; 30 min, 30% A; 32 min, 0% A; and 35 min, 100% A. Wavelengths were detected at 306 and 360 nm for hyperoside and quercetin, respectively. Standard compounds for the identification and quantitative analysis of hyperoside and quercetin were obtained from Acros Organics (Morris Plains, NJ, USA).

Oxygen radical absorbance capacity. The antioxidant capacity was determined using an oxygen radical absorbance capacity assay (ORAC) with fluorescein as the fluorescent probe using a FLUOstar fluorescent microplate reader (485 nm excitation and 538 nm emission; BMG Labtech Inc., Cary, NC, USA). Results are expressed in μmol of Trolox equivalents/ml.

Cell culture. Hormone-independent PC3 prostate cancer epithelial cell lines were purchased from the American Type Culture Collection (Manassas, VA, USA). Cells were cultured at 37˚C with 5% CO_2 in RPMI-1640 (Gibco-BRL, Carlsbad, CA, USA) supplemented with 10% fetal bovine serum (FBS; Gibco-BRL), penicillin (100 IU/ml; Gibco-BRL) and streptomycin (100 μg/ml; Gibco-BRL).

Generation of ROS. ROS production was determined using the 2',7'-dichlorofluorescein diacetate (DCFH-DA; Eastman Kodak, Rochester, NY, USA) assay according to the manufacturer's instructions. In brief, cells were seeded in a clear-bottom, 96-well plate ($1x10^4$ cells/well), incubated for 24 h and then treated with different concentrations of QH (0-60 μg/ml). Following incubation, cells were washed twice with phosphate-buffered saline (PBS) and incubated with 200 μM hydrogen peroxide for 2 h at 37˚C. Cells were then washed with PBS in order to remove hydrogen peroxide and 10 μM DCFH-DA diluted in PBS was added to cells, followed by incubation for 15 min at 37˚C. DCFH-DA was removed and fluorescence intensity was measured using a FLUOstar fluorescent microplate reader as described above.

Cell viability assay. Prostate cancer cells were seeded in a 96-well plate ($3x10^3$ cells/well) and incubated for 24 h. The growth medium was then replaced with the experimental medium containing various concentrations of QH extract (0-60 μg/ml). Cell viability was assessed at 48 and 72 h using a Cell Titer 96® AQueous One Solution Cell Proliferation assay kit (Promega Corp., Madison, WI, USA) according to manufacturer's instructions, and a FLUOstar microplate reader at 490 nm. The IC_{50}-value was calculated using sigmoidal nonlinear regression analyses of the percentage of cell inhibition as a ratio of the control using GraphPad Prism 5.01 (GraphPad Software, Inc., La Jolla, CA, USA).

Cell proliferation. Prostate cancer cells were cultured in a 24-well plate ($2x10^4$ cells/well) for 24 h. The growth medium was then replaced with the experimental medium containing numerous concentrations of QH extract (0-60 μg/ml). Cell proliferation was determined following 48 and 72 h incubation using a cell counter (Beckman Coulter LH500, Brea, CA, USA). Cell counts were expressed as a percentage of the control cells.

Cell apoptosis. The rate of apoptotic cell death was determined using a fluorescein isothiocyanate (FITC)-Annexin V apoptosis detection kit (BD Pharmingen, San Diego, CA, USA) according to the manufacturer's instruction and quantified using flow cytometry. In brief, following treatment of prostate cancer cells with QH for 24 h, cells were washed once with PBS and harvested in a 0.5% trypsin/EDTA solution at 37˚C, centrifuged at 500 x g for 5 min and then immediately re-suspended in 1X physiological buffer (provided in the kit). Cells ($1x10^5$/500 μl) were then maintained in the dark for 15 min at room temperature with 5 μl each of propidium iodide and FITC conjugated Annexin V solution (Promega Corp.). The samples were then analyzed using a FACSCalibur flow cytometer (BD Biosciences, San Jose, CA, USA). Results were quantified using CellQuest software (BD Biosciences, San Jose, CA).

Cleaved caspase-3 activation. Cells ($6x10^5$/well) were cultured for 24 h and then incubated with numerous concentrations of QH (0-40 μg/ml) for 24 h. Cleaved caspase-3 activation was determined using an ELISA kit (Cell Signaling Technology Inc., Danvers, MA, USA) according to the manufacturer's instructions and quantified using a FLUOstar microplate reader at 450 nm.

Cell cycle analysis. Prostate cancer cells were seeded in a 12-well plate ($5x10^4$ cells/well) with medium containing 2.5% FBS for 24 h. Cells were then treated with QH (0-40 μg/ml) for 24 h. Cells were fixed with 90% ethanol and stored at -20˚C. DNA was stained using propidium iodide (PI; Promega Corp.) containing a 0.2 mg/ml RNAse solution and analysis was performed at 488 nm excitation and 620 nm emission using a FACSCalibur flow cytometer. The percentage of cells in each cell cycle phase was analyzed using ModFit LT version 3.2 for Macintosh (Verity Software House Inc., Topsham, ME, USA).

Wound-healing assay. Equal numbers of cells were seeded into each well of a 12-well culture plate. Cells were incubated until they reached 70-80% confluence and a wound was created by scratching a line down the middle of the well using a sterile white pipette tip. Cells were then treated with different concentrations of QH and incubated for 48 hours. Differential interference contrast images of the wounded area were captured of three random fields per well using a microscope (Nikon E-600 microscope; Nikon, Inc., Melville, NY, USA) at 0 and 48 h post-wounding. Wound-healing was quantified by measuring the area of the closing wound, which was normalized to that of the vehicle-treated controls.

Invasion assay. Prostate cancer cell migration through Matrigel-coated membranes was measured using a 24-well BD Biocoat Matrigel® invasion chamber (BD Biosciences). Prostate cancer cells ($5x10^4$) were suspended in culture media without serum and then seeded onto the top compartment of the invasion chamber, followed by respective QH treatments. Complete media was added to the bottom chamber. Following 48 h, the cell inserts were obtained and cells were removed from the top surface of the membrane using a cotton swab. The invasive cells adhering to the bottom surface of the membrane were stained using 100% methanol (Sigma-Aldrich) and 1% toluidine blue (Sigma-Aldrich), respectively. Images were captured under a light microscope using a 20x objective. The total number of invaded cells was manually counted in four randomly selected fields per treatment per insert.

Reverse transcription quantitative polymerase chain reaction analysis (RT-qPCR) of miRNA and mRNA. Prostate cancer cells were cultured in a six-well plate ($2x10^5$ cells/well) for 24 h prior to incubation with different concentrations of QH (0-30 μg/ml). Total RNA, containing mRNA and miRNA, was isolated using the mirVana™ miRNA Isolation kit (Applied Biosystems, Foster City, CA, USA) according to the manufacturer's instructions. Extracted nucleic acid was evaluated qualitatively and quantitatively using the NanoDrop® ND-1,000 Spectrophotometer (NanoDrop Technologies Inc., Wilmington, DE, USA) at 260 and 280 nm. SuperScript™ III First-Strand (Invitrogen Life Technologies, Carlsbad, CA, USA) was used to reverse-transcribe mRNA. GAPDH was used as a qPCR endogenous control. qPCR for mRNA was performed using the SYBR Green ER qPCR SuperMix (Invitrogen Life Technologies) on a 7900HT Fast Real-Time PCR System (Applied Biosystems). Primers used for RT-qPCR were as follows: PDCD4 sense, 5'-CCAAAGAAAGGTGGTGCA-3' and antisense, 5'-TGAGGTACTTCCAGTTCC-3'; GAPDH sense, 5'-GGCATTGCTCTCAATGACAA-3' and antisense, 5'-ATGTAGGCCATGAGGTCCAC-3'.

The TaqMan® MicroRNA Assay for miR-21 and the control RNU6B (Applied Biosystems) was used according to the manufacturer's instructions, to reverse-transcribe mature miRNA in a MasterCycler (Eppendorf, Hamburg, Germany). RT-qPCR for miRNA was performed using the TaqMan® assay, which contained the forward and reverse primers as well as the TaqMan® probe and TaqMan® Universal PCR Master Mix No AmpErase® uracil *N*-glycosylase (Applied Biosystems). Quantification of mRNA and miRNA gene expression was then evaluated using the comparative critical threshold method. Mimic transfections with 50 and 100 nM miR-21 (Dharmacon, Lafayette, CO, USA) were performed using Lipofectamine 2000® (Invitrogen Life Technologies) for 6 h. Following transfection, cells were incubated with 20 μg/ml QH for 24 h.

Western blot analysis. Cells were cultured ($2x10^6$ cells/plate) for 24 h and then incubated with different concentrations of QH for 48 h. Cells were lysed in lysis buffer containing protease inhibitor. Protein concentration was determined using a Bio-Rad protein assay system (Bio-Rad, Hercules, CA, USA). Equal amounts of proteins were separated using SDS-PAGE on a 15% gel and then transferred onto polyvinylidene difluoride membranes (Bio-Rad). Following blocking in Tris-buffered saline containing 5% non-fat milk, the membranes were incubated with specific primary antibodies (mouse anti-PDCD4 polyclonal antibody, dilution 1:1,000, Abnova Corporation, Walnut, CA, USA; and mouse anti-PARP polyclonal antibody, dilution 1:1,000, Abcam, Cambridge, MA, USA) at 4˚C for 12 h and then with horseradish peroxidase-conjugated anti-mouse secondary antibody for 2 h at room temperature. Enhanced chemiluminescence detection reagent (GE Healthcare, Little Chalfont, UK) was used to evaluate the results.

Statistical analysis. Data from *in vitro* experiments were analyzed by one-way analysis of variance followed by a Tukey-Cramer HSD multiple comparison test using SPSS version 18.0 (International Business Machines, Armonk, NY, USA). A Student t-test was used to determine differences between miR-21 mimic transfections. Nonlinear modeling of sigmoidal curves for cell viability was performed using GraphPad Prism 5.01. $P<0.05$ was considered to indicate a statistically significant difference between values.

Results

Chemical composition. As shown in Fig. 1A and C, the chromatographic stilbene and flavonal profiles of QH, respectively, demonstrated the presence of two major polyphenols, hyperoside (peak 1) and quercetin (peak 2) in this botanical supplement. The chemical structures of hyperoside and quer-

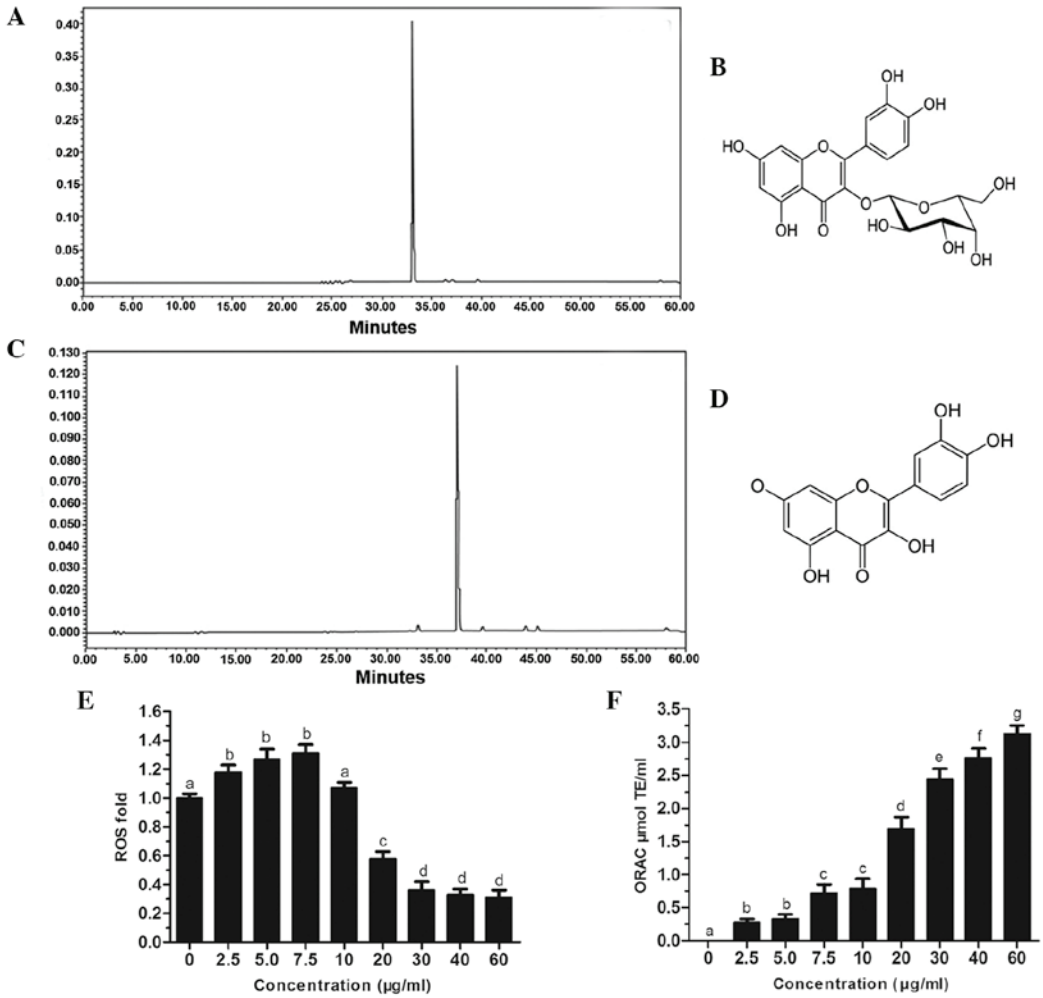

Figure 1. Chromatographic profiles of the QH mixture with detection at different wavelengths and the effect of different concentrations of QH on ROS and antioxidant levels in PC3 cells. (A and C) Chromatographic profiles of the stilbene hyperoside (detection at 306 nm) and the flavonol quercetin (detection at 360 nm) in QH. (B and D) Chemical structures of hyperoside and quercetin, respectively. (E) Hydrogen peroxide-induced generation of ROS in PC3 cells treated with different concentrations of QH for 24 h. (F) ORAC-values of PC3 cells treated with different concentrations of QH for 24 h. Values are presented as the mean ± standard error of the mean (n=3). Least significant difference tests were performed and bars with different letters are significantly different ($P<0.05$). QH, hyperoside and quercetin in combination; ROS, reactive oxygen species; ORAC, oxygen radical absorbance capacity assay, TE, Trolox equivalents.

cetin are shown in Fig. 1B and D, respectively. In addition, quercetin and hyperoside were reported to be among the most abundant flavonoids in a standard human diet (5,18).

Production of intracellular ROS and ORAC. Intracellular production of ROS was investigated in PC3 cells following treatment with hydrogen peroxide. The results revealed that at low concentrations of QH (0-10 μg/ml), there was a slight increase in ROS production; however, at higher concentrations of QH (20-60 μg/ml), ROS production was significantly decreased by up to 69% compared to that of the control cells (Fig. 1E). An ORAC assay was then used to determine the antioxidant capacity of cells following QH treatment (Fig. 1F). The results demonstrated that all tested concentrations of QH significantly increased the antioxidant capacity of PC3 cells in a dose-dependent manner.

QH inhibits PC3 cell viability. A Cell Titer 96® cell proliferation assay was used to determine cell viability following incubation with different concentrations of QH for 48 and 72 h. The results demonstrated that QH significantly decreased PC3 cell viability in a dose- and time-dependent manner (Fig. 2A), with IC_{50}-values of 19.7 and 12.4 μg/ml, for 48 and 72 h, respectively. In addition, determination of the cell count of PC3 cells showed that QH significantly inhibited the proliferation of PC3 cells following 48 and 72 h of treatment with QH in a dose- and time-dependent manner (Fig. 2B). The total cell count was significantly decreased at all tested concentrations (2.5-60 μg/ml) and at 60 μg/ml, QH cell proliferation was reduced by 76 and 85%, following 48 h and 72 h of incubation, respectively.

As shown in Fig. 2C, the effects of QH on cell-cycle progression were determined by fluorescence-activated cell sorting analysis. No significant changes were observed in the percentage of cells in different phases of the cell cycle; however, there was a significant G0/G1 to S phase block compared to control cells following treatment with 10, 20 and 40 μg/ml QH (Fig. 2C).

Annexin V-FITC and propidium iodide staining and flow cytometric analysis determined that QH increased apoptosis in PC3 cells at all tested concentrations (2.5-40 μg/ml) compared

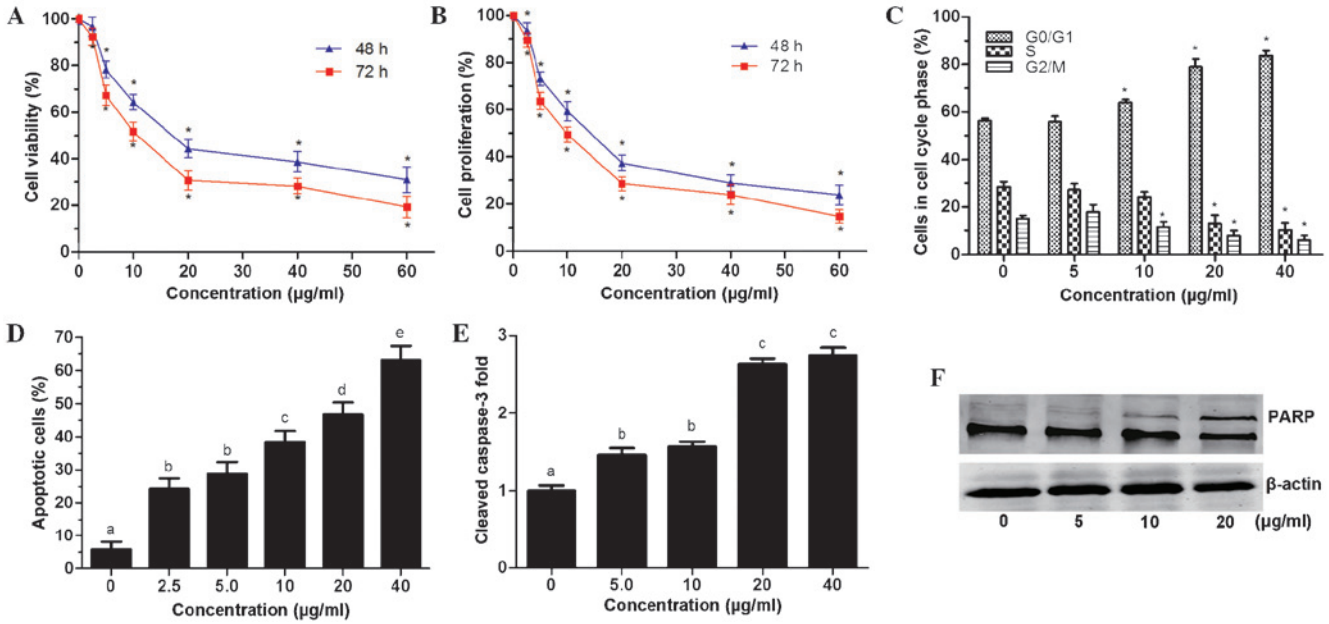

Figure 2. Effects of QH on cell viability, proliferation and apoptosis of PC3 cells. (A) Cell viability and (B) proliferation rate of PC3 cells treated with different concentrations of QH (0-60 μg/ml) for 48 and 72 h. (C) Cell cycle kinetics and (D) apoptotic rate of PC3 cells treated with different concentrations of QH (0-40 μg/ml) for 24 h. (E) ELISA was used to determine protein levels of cleaved caspase-3 in PC3 cells treated with different concentrations of QH (0-40 μg/ml) for 24 h. (F) Protein expression of PARP-1 and cleaved PARP in PC3 cells treated with different concentrations of QH (0-20 μg/ml) for 48 h. β-actin was used as the internal control. Values are presented as the mean ± standard error of the mean (n=3). Least significant difference tests were performed, bars with different letters are significantly different (P<0.05). QH, hyperoside and quercetin in combination; PARP, poly(adenosine diphosphate ribose) polymerase.

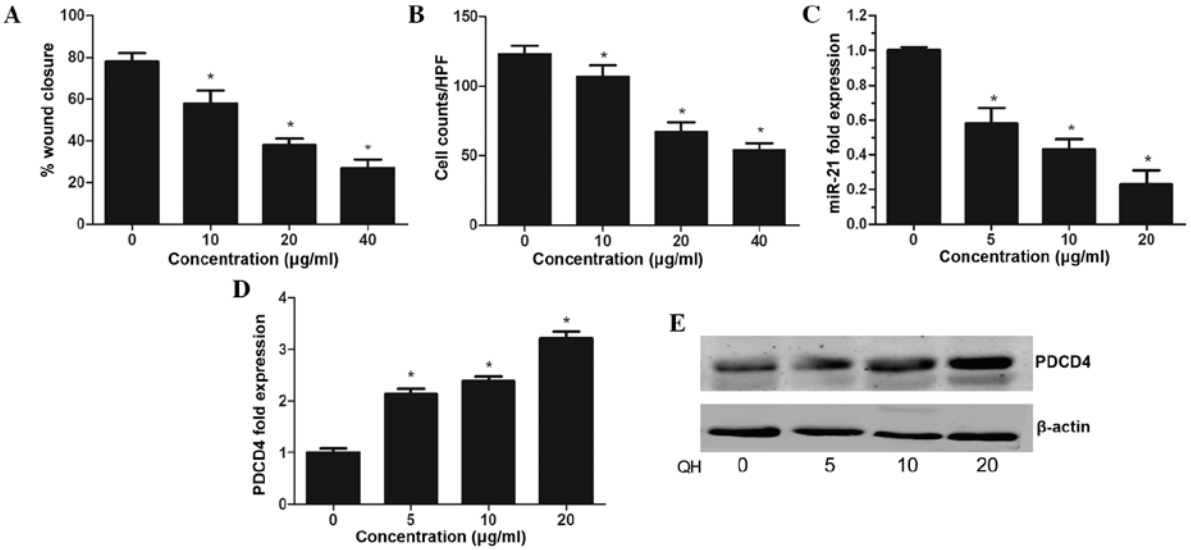

Figure 3. Effects of QH on invasion activity as well as miR-21 and PDCD4 expression in PC3 cells. (A) Wound healing assays and (B) modified Boyden invasion chamber assays revealed that treatment with different concentrations of QH for 48 h significantly inhibited PC3 cell invasion. (C) Reverse transcription quantitative polymerase chain reaction using TaqMan® miRNA assay following incubation of PC3 cells with different concentrations of QH for 24 h was performed in order to determine (C) miR-21 and (D) PDCD4 expression levels. (E) Western blot analysis of PDCD4 protein expression levels in PC3 cells following treatment with different concentrations of QH for 48 h. β-actin was used as the internal control. Values are presented as the mean ± standard error of the mean (n=3). *P<0.05 vs. control. QH, hyperoside and quercetin in combination; miR/miRNA, micro RNA; PDCD4, programmed cell death 4.

to that in the control, with a maximum increase at 40 μg/ml QH by 63% (Fig. 2D).

Furthermore, activated/cleaved caspase-3 levels were found to be elevated at low concentration of QH (5 and 10 μg/ml) by ~1.5-fold and at higher concentrations (20 and 40 μg/ml) by ~2.7-fold (Fig. 2E). Poly(adenosine diphosphate ribose) polymerase 1 (PARP-1) is a substrate for caspase-3 cleavage, which produces cleaved PARP-1 (19). In the present study, western blot analysis revealed an increase in PARP cleavage in PC3 cells following QH treatment (Fig. 2F). These results therefore indicated that cleaved caspase-3 was activated and had a role in the induction of apoptosis following QH treatment.

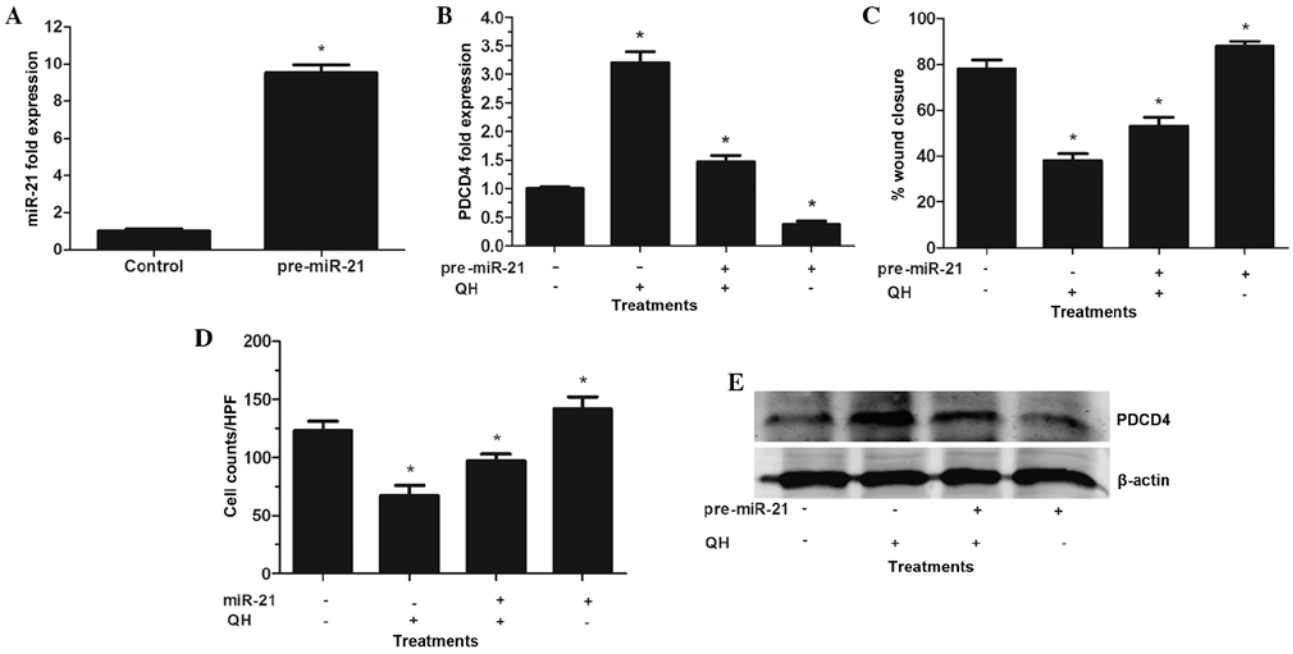

Figure 4. Pre-miR-21 increases the levels of miR-21 and attenuates QH-induced anti-cancer activity. Reverse transcription quantitative polymerase chain reactions using TaqMan® miRNA assay was used to determine expression of (A) miR-21 in PC3 cells following transfection of pre-miR-21 for 48 h and (B) PDCD4 in PC3 cells following transfection of pre-miR-21 and treatment with 20 mg/ml QH for 24 h. (C) Wound healing assays and (D) modified Boyden invasion chamber assays were performed in order to show the effect of transfection of pre-miR-21 and treatment with 20 mg/ml QH for 48 h on PC3 cell migration and invasion activity. (E) Western blot analysis of PDCD4 expression levels in PC3 cells following transfection of pre-miR-21 and treatment with 20 mg/ml QH for 48 h. β-actin was used as the internal control. Values are presented as the mean ± standard error of the mean (n=3). *P<0.05 vs. control. QH, hyperoside and quercetin in combination; miR/miRNA, micro RNA; PDCD4, programmed cell death protein4.

QH inhibits the invasive activity of PC3 cells. The present study aimed to investigate the effect of QH on prostate cancer cell migration and invasion. The results of the wound healing assay demonstrated that QH-treated PC3 cells had significantly decreased migratory ability compared to that of the control (P<0.05) (Fig. 3A). A Matrigel® invasion assay determined that the average cell counts crossing a Matrigel®-coated membrane in the control group was significantly increased compared to that of the QH treatment group, indicating that QH significantly suppressed the invasive capacity of prostate cancer cells (P<0.05) (Fig. 3B).

QH regulates miR-21 expression in PC3 cells. A TaqMan® assay was performed in order to evaluate the expression of miR-21 in PC3 cells following QH treatment. The results showed a dose-dependent decrease in miR-21 expression, with inhibition rates of 42, 56 and 77% observed at 5, 10 and 20 μg/ml QH, respectively (Fig. 3C). In addition, a dose-dependent increase in PDCD4 expression, a target molecule for miR-21, was detected in PC3 cells following treatment with QH (Fig. 3D and E). This therefore indicated that the mechanisms underlying the anti-cancer effect of QH in PC3 cells may proceed via the suppression of the miR-21 gene.

PC3 cells were then transfected with pre-miR-21 in order to induce the overexpression of miR-21. Pre-miR-21 is processed by the RNAse III enzyme Dicer, which results in a 22 base pair double-stranded RNA with two nucleotide 39 overhangs; one of these strands forms the mature miRNA, which is incorporated into an RNA silencing complex (RISC), allowing it to functionally suppress the expression and translation of its targeted RNAs (20). In the present study, increased miR-21 levels compared to those in the control-transfected cells confirmed the effectiveness of miR-21 transfection (Fig. 4A). As hypothesized, PDCD4 levels were significantly decreased compared to those of the control, indicating that miR-21 bound to the 3' untranslated region on PDCD4 mRNA and enhanced its degradation (15). These results suggested that pre-miR-21 was effectively processed in PC3 cells, resulting in the functional overexpression of miR-21. Furthermore, the overexpression of pre-miR-21 resulted in partial resistance of transfected PC3 cells to QH-induced PDCD4 stimulation (Fig. 4B and E). However, QH retained its ability to augment PDCD4 levels in cells via the suppression of the high basal miR-21 expression. In addition, cells overexpressing miR-21 exhibited an increased resistance to QH-induced suppression of PC3 cells wound healing and invasive capacity (Fig. 4C and D). In conclusion, the results of these experiments indicated that miR-21 was the target gene for QH treatment, which mediated the growth and invasiveness of PC3 cells *in vitro*.

Discussion

The production of ROS is known to be associated with the oxidative cellular damage involved in the development of numerous pathological conditions (21). ROS have a complex role in carcinogenesis; the majority of cancer cells have increased constitutive levels of ROS compared to those of normal cells, due to mutations in nuclear and mitochondrial genes responsible for the electron transport chain as well as increased metabolic and mitochondrial activity (22). It was reported that elevated ROS levels may enhance cell proliferation among other events associated with cancer progression (23). In addition, ROS were

reported to induce DNA damage and oxidation of fatty acids in cellular membrane structures, which may facilitate mutagenesis and cancer development. However, numerous anti-cancer drugs are toxic to mitochondria and induce ROS production, which may in turn lead to cancer cell death (24). Polyphenols, including hyperoside and quercetin, have the ability to scavenge free radicals and induce the activation of antioxidant and detoxifying enzymes, therefore protecting cells against oxidative damage caused by carcinogenic compounds (25). In the present study, QH induced a dose-dependent increase in the intracellular antioxidant capacity; by contrast, low concentrations of QH increased ROS production in PC3 cells, whereas high concentrations significantly reduced ROS levels. One possible explanation for this biphasic effect may be the toxic effects of polyphenols in mitochondria, which may have induced ROS production, whereas at higher concentrations of QH, their antioxidant properties became dominant (25). Previous studies have demonstrated the protective effect of polyphenols against oxidative damage under certain conditions (26). This may indicate that in the present study, the lower concentrations of QH were insufficient to have protective effects and therefore resulted in the additional formation of radicals, whereas at higher concentrations, QH inhibited ROS production, potentially through scavenging ROS.

The anti-proliferative effects of quercetin were previously demonstrated in MOLT-4 leukemia cells through the combination of resveratrol and quercetin, which exhibited synergistic anti-cancer effects (12). Based on previous studies, a combination of hyperoside and quercetin (ratio, 1:1) was investigated in the present study, resulting in significant decrease in cell viability and proliferation following QH treatment. However, it remains to be elucidated whether a different ratio may be more effective.

A previous study demonstrated that polyphenols, including resveratrol and quercetin, induced cell cycle arrest in numerous cancer cell lines at different phases (27). Tan *et al* (28) studied the effect of quercetin on HepG2 cells and reported that following treatment with quercetin for 48 h, cells were arrested in G0/G1 phase. In MOLT-4 leukemia cells, polyphenol-mediated cell cycle arrest was influenced by the duration of treatment and the type of polyphenol. In the present study, QH (20 μg/ml) decreased the percentage of cells in S-phase and increased the percentage of cells in G0/G1-phase, which was consistent with the inhibition of the progression from G0/G1 to S-phase.

Caspase-3 is an important enzyme in apoptosis and a commonly used indicator for the induction of apoptosis (28). PARP-1, an abundant chromatin-associated protein, has a significant role in maintaining genome integrity and is cleaved by caspase-3 during apoptosis (29). Previous studies have demonstrated the effects of quercetin, as well as other polyphenols, on caspase-3 and PARP-1 activity (30,31). In general, the results of the present study are in accordance with those of previous studies, which showed that polyphenols induced apoptosis via the activation of caspase-3 accompanied by cleavage of PARP (28). These previous studies also reported that resveratrol caused the induction of caspase-3 and PARP cleavage in human articular chondrocytes and myeloid leukemia cells.

The results of the present study indicated that the miR-21 axis was an important target of QH for mediating the survival and invasive capacity of PC3 prostate cancer cells. It was found that the underlying mechanism of QH anti-cancer activity was via the induction of miR-21 targeted genes, such as PDCD4. In addition, the present study demonstrated that overexpression of miR-21 antagonized the anti-tumor effects of QH, which further highlighted the role of the miR-21 pathway in mediating the anti-tumor actions of QH in prostate cancer cells.

miR-21 is an oncomir which has an important role in regulating numerous cellular processes in order to enhance cancer cell growth and invasion. Expression of miR-21 is high in androgen-independent prostate cancer cell lines, including PC3 and DU145, and low in androgen-dependent prostate cancer cells, such as LNCaP cells (32). It was hypothesized that the androgen/androgen receptor complex binds to the promoter region of miR-21 in order to induce its expression (33). Of note, the resultant high expression of miR-21 was suggested to promote androgen resistance via downstream gene regulation; miR-21-regulated genes include myristoylated alanine-rich protein kinase c substrate (MARCKS), PDCD4, maspin and tropomyosin-1 (20,34). miR-21 has been reported to negatively regulate MARCKS, which was suggested to control cell motility through interactions with the actin cytoskeleton (32). It was subsequently reported that cells treated with antisense miR-21 exhibited increased MARCKS expression and reduced invasive capacity (35). Downregulation of MARCKS using siRNAs increased the invasiveness of DU-145 prostate cancer cells (32).

The anti-tumor activity of PDCD4 was suggested to proceed through numerous mechanisms; PDCD4 was reported to suppress protein translation via inhibition of the eukaryotic initiation factor 4A activity (36). In addition, PDCD4 suppressed the transactivation of the activator protein (AP)-1 promoter via c-Jun (37), therefore inhibiting growth promotion. These previous studies provided evidence to support the conclusion that QH inhibited miR-21 expression in PC3 cells and increased the expression of key target proteins, such as PDCD4; furthermore, overexpression of miR-21 decreased the expression of the miR-21 target PDCD4 and reduced the ability of QH to mediate the invasive capacity of PC3 cells.

In conclusion, the results of the present study indicated that a combination of quercetin and hyperoside exhibited anti-tumor activities in prostate cancer cells, resulting in apoptosis, cell cycle arrest and reduced invasive capacity. QH-induced regulation of the miR-21-PDCD4 axis was identified as one possible underlying mechanism of the anti-cancer effects of QH. Further studies are required in order to assess the role and clinical relevance of miRNA-21 in the anti-cancer effects exhibited by botanicals.

Acknowledgements

This work was partially supported by grants from the National Natural Science Foundation of China (nos. 81000311 and 81270831).

References

1. Siegel R, Naishadham D and Jemal A: Cancer statistics, 2013. CA Cancer J Clin 63: 11-30, 2013.
2. Mottet N, Bellmunt J, Bolla M, *et al*: EAU guidelines on prostate cancer. Part II: Treatment of advanced, relapsing, and castration-resistant prostate cancer. Actas Urol Esp 35: 565-579, 2011 (In Spanish).

3. Chuu CP, Kokontis JM, Hiipakka RA, *et al*: Androgens as therapy for androgen receptor-positive castration-resistant prostate cancer. J Biomed Sci 18: 63, 2011.
4. Harzstark AL and Small EJ: Castrate-resistant prostate cancer: therapeutic strategies. Expert Opin Pharmacother 11: 937-945, 2010.
5. Theodoratou E, Kyle J, Cetnarskyj R, *et al*: Dietary flavonoids and the risk of colorectal cancer. Cancer Epidemiol Biomarkers Prev 16: 684-693, 2007.
6. Choi JA, Kim JY, Lee JY, *et al*: Induction of cell cycle arrest and apoptosis in human breast cancer cells by quercetin. Int J Oncol 19: 837-844, 2001.
7. Kim MJ, Kim YJ, Park HJ, Chung JH, Leem KH and Kim HK: Apoptotic effect of red wine polyphenols on human colon cancer SNU-C4 cells. Food Chem Toxicol 44: 898-902, 2006.
8. Tang SN, Singh C, Nall D, Meeker D, Shankar S and Srivastava RK: The dietary bioflavonoid quercetin synergizes with epigallocathechin gallate (EGCG) to inhibit prostate cancer stem cell characteristics, invasion, migration and epithelial-mesenchymal transition. J Mol Signal 5: 14, 2010.
9. Srivastava RK, Tang SN, Zhu W, Meeker D and Shankar S: Sulforaphane synergizes with quercetin to inhibit self-renewal capacity of pancreatic cancer stem cells. Front Biosci (Elite Ed) 3: 515-528, 2011.
10. Zou Y, Lu Y and Wei D: Antioxidant activity of a flavonoid-rich extract of *Hypericum perforatum* L. *in vitro*. J Agric Food Chem 52: 5032-5039, 2004.
11. Gao LL, Feng L, Yao ST, *et al*: Molecular mechanisms of celery seed extract induced apoptosis via s phase cell cycle arrest in the BGC-823 human stomach cancer cell line. Asian Pac J Cancer Prev 12: 2601-2606, 2011.
12. Mertens-Talcott SU, Talcott ST and Percival SS: Low concentrations of quercetin and ellagic acid synergistically influence proliferation, cytotoxicity and apoptosis in MOLT-4 human leukemia cells. J Nutr 133: 2669-2674, 2003.
13. George J, Singh M, Srivastava AK, *et al*: Resveratrol and black tea polyphenol combination synergistically suppress mouse skin tumors growth by inhibition of activated MAPKs and p53. PLoS One 6: e23395, 2011.
14. Farazi TA, Spitzer JI, Morozov P and Tuschl T: miRNAs in human cancer. J Pathol 223: 102-115, 2011.
15. Si ML, Zhu S, Wu H, Lu Z, Wu F and Mo YY: miR-21-mediated tumor growth. Oncogene 26: 2799-2803, 2007.
16. Zhu S, Wu H, Wu F, Nie D, Sheng S and Mo YY: MicroRNA-21 targets tumor suppressor genes in invasion and metastasis. Cell Res 18: 350-359, 2008.
17. Chen Y, Liu W, Chao T, *et al*: MicroRNA-21 down-regulates the expression of tumor suppressor PDCD4 in human glioblastoma cell T98G. Cancer Lett 272: 197-205, 2008.
18. Frémont L: Biological effects of resveratrol. Life Sci 66: 663-673, 2000.
19. Brauns SC, Dealtry G, Milne P, Naudé R and Van de Venter M: Caspase-3 activation and induction of PARP cleavage by cyclic dipeptide cyclo(Phe-Pro) in HT-29 cells. Anticancer Res 25: 4197-4202, 2005.
20. Selcuklu SD, Donoghue MT and Spillane C: miR-21 as a key regulator of oncogenic processes. Biochem Soc Trans 37 (Pt 4): 918-925, 2009.
21. Carew JS and Huang P: Mitochondrial defects in cancer. Mol Cancer 9: 9, 2002.
22. Fresco P, Borges F, Diniz C and Marques MP: New insights on the anticancer properties of dietary polyphenols. Med Res Rev 26: 747-766, 2006.
23. Schumacker PT: Reactive oxygen species in cancer cells: live by the sword, die by the sword. Cancer Cell 10: 175-176, 2006.
24. Ling YH, Liebes L, Zou Y and Perez-Soler R: Reactive oxygen species generation and mitochondrial dysfunction in the apoptotic response to Bortezomib, a novel proteasome inhibitor, in human H460 non-small cell lung cancer cells. J Biol Chem 278, 33714-33723, 2003.
25. Biasutto L, Szabo' I, Zoratti M. Mitochondrial effects of plant-made compounds. Antioxid Redox Signal 15: 3039-3059, 2011.
26. Hsu SC, Lu JH, Kuo CL, *et al*: Crude extracts of *Solanum lyratum* induced cytotoxicity and apoptosis in a human colon adenocarcinoma cell line (colo 205). Anticancer Res 28 (2A): 1045-1054, 2008.
27. Schlachterman A, Valle F, Wall KM, *et al*: Combined resveratrol, quercetin, and catechin treatment reduces breast tumor growth in a nude mouse model. Transl Oncol 1: 19-27, 2008.
28. Tan J, Wang B and Zhu L: Regulation of survivin and Bcl-2 in HepG2 cell apoptosis induced by quercetin. Chem Biodivers 6: 1101-1110, 2009.
29. Shakibaei M, John T, Seifarth C and Mobasheri A: Resveratrol inhibits IL-1 beta-induced stimulation of caspase-3 and cleavage of PARP in human articular chondrocytes *in vitro*. Ann NY Acad Sci 1095: 554-563, 2007.
30. Wang ZQ, Stingl L, Morrison C, *et al*: PARP is important for genomic stability but dispensable in apoptosis. Genes Dev 11: 2347-2358, 1997.
31. Hsu CP, Lin YH, Chou CC, *et al*: Mechanisms of grape seed procyanidin-induced apoptosis in colorectal carcinoma cells. Anticancer Res 29: 283-289, 2009.
32. Li T, Li D, Sha J, Sun P and Huang Y: MicroRNA-21 directly targets MARCKS and promotes apoptosis resistance and invasion in prostate cancer cells. Biochem Biophys Res Commun 383: 280-285, 2009.
33. Ribas J, Ni X, Haffner M, *et al*: miR-21: an androgen receptor-regulated microRNA that promotes hormone-dependent and hormone-independent prostate cancer growth. Cancer Res 69: 7165-7169, 2009.
34. Pang Y, Young CY and Yuan H: MicroRNAs and prostate cancer. Acta Biochim Biophys Sin (Shanghai) 42: 363-369, 2010.
35. Arbuzova A, Schmitz AA and Vergères G: Cross-talk unfolded: MARCKS proteins. Biochem J 362 (Pt 1): 1-12, 2002.
36. Yang HS, Jansen AP, Komar AA, *et al*: The transformation suppressor Pdcd4 is a novel eukaryotic translation initiation factor 4A binding protein that inhibits translation. Mol Cell Biol 23: 26-37, 2003.
37. Bitomsky N, Böhm M and Klempnauer KH: Transformation suppressor protein Pdcd4 interferes with JNK-mediated phosphorylation of c-Jun and recruitment of the coactivator p300 by c-Jun. Oncogene 23: 7484-7493, 2004.